

## EXPERIMENTATION AND MODELLING FOR *COLOCASIA ESCULENTA* (L.) *SCHOOT* SLICES DRYING PROCESS

Ai S. Zhu\*, Yan W. Shi, Da Z. Tao, Mao Q. Xu, Jun Z. Zhao

*Zhejiang University of Science and Technology, School of Biological and  
Chemical Engineering, 318 Liuhe Road, Hangzhou, China*

\*Corresponding author: [939454044@qq.com](mailto:939454044@qq.com), [zhuaishi86@163.com](mailto:zhuaishi86@163.com)

Received: May, 12, 2018

Accepted: April, 22, 2019

**Abstract:** The effects of drying air temperature, air velocity and slices thickness on the drying behavior of *Colocasia esculenta* (L.) *Schoot* slices were investigated in a convective hot air tunnel dryer. Mass transfer during the drying was described using six models and the models performances were evaluated. The effective diffusion coefficients ( $D_{\text{eff}}$ ) were calculated and the temperature dependency of  $D_{\text{eff}}$  was illustrated. The results showed that the drying took place in main falling rate period; the Logarithmic model showed good agreement with all experiments data; at the varied range of temperature the  $D_{\text{eff}}$  values varied from  $4.94 \times 10^{-10}$  to  $6.86 \times 10^{-10} \text{ m}^2 \cdot \text{s}^{-1}$  and it fitted the Arrhenius equation, the activation energy was  $16.15 \text{ kJ} \cdot \text{mol}^{-1}$ ; with the increase of hot air velocity from 0.5 to  $1.5 \text{ m} \cdot \text{s}^{-1}$ , the  $D_{\text{eff}}$  varied from  $4.51 \times 10^{-10}$  to  $6.68 \times 10^{-10} \text{ m}^2 \cdot \text{s}^{-1}$ ; for slices thickness 1, 2 and 3 mm, the  $D_{\text{eff}}$  was  $1.69 \times 10^{-10}$ ,  $5.76 \times 10^{-10}$  and  $9.81 \times 10^{-10} \text{ m}^2 \cdot \text{s}^{-1}$  respectively.

**Keywords:** *activation energy, Colocasia esculenta* (L.) *Schoot*, *convective hot air drying, effective diffusion coefficient, modelling*

## INTRODUCTION

*Colocasia esculenta* (L.) Schott is a tropical plant grown primarily for its edible corms, the root vegetables whose many names include taro and eddoe. It is believed to be one of the earliest cultivated plants. Its tuber contain not only the common nutrients, such as starch, protein, lipid and crude fiber, but it is also rich in calcium, potassium, phosphorus, zinc, magnesium, iron, and vitamin B, C [1, 2]. *Colocasia esculenta* (L.) Schott, commonly known as taro, is an essential food for millions of people. The leaves are consumed in sauces, purees, stews, and soups [3]. Taro corms and leaves are also accredited to have medicinal value and are used to reduce tuberculoses, ulcers, pulmonary congestion and fungal infection [4]. The Food and Agriculture Organization estimates that 9.1 million Mt of corms are produced annually on a surface of 2 million ha. *Colocasia esculenta* (L.) Schott is decayed and deteriorated due to their high moisture content. The processing of fresh *Colocasia esculenta* (L.) Schott tuber becomes very significant.

Drying is likely the earliest and the most important preserving method of agricultural products and foods known and used well by humans [5]. The primary aim of agricultural products and foods drying is the extended of the safe store period through the reduction of their moisture content to a level, in addition also could reduce the volume and quality through drying and then lower the expenses of products packaging, shipping and storing [6]. The method of hot air drying proceeding in equipment could ensure the drying process to be fast, drying environment to be hygienic and product to be safe and uniform, so it suits for industrialization of agricultural products and foods drying [7]. The importance of the drying kinetics knowledge is obvious for the development of drying models, knowing of the mechanisms of moisture transfer, optimization of process conditions, and design of drying method and equipment [8]. There have been many studies on the drying model and the drying performance of various agricultural products, such as sweet potato [5], sweet cherry [6], seedless grapes [7], organic tomato [8], potato [9], yam [10], carrots [11], etc. Literature reports that scholars researched the chemical composition of *Colocasia esculenta* (L.) Schott and its properties [1 – 4].

However, there is no report on the effects of air temperature, air velocity and thickness of slices for the drying process of *Colocasia esculenta* (L.) Schott and the modelling of drying process in convective hot air drying tunnel.

The aims of this research were:

- (1) to observe the influences of air temperature, air velocity and thickness of slices on the drying time and dehydration rate;
- (2) to fit the experimental data to six thin-layer drying models, evaluate models and estimate the constants;
- (3) to calculate the effective diffusion coefficient and activation energy from Fick's second law and Arrhenius equation, for drying of *Colocasia esculenta* (L.) Schott.

## MATERIALS AND METHODS

### Sample preparation and pretreatment

Uniform (about 4 - 5 cm in largest diameter and about 7 - 8 cm in length) fresh *Colocasia esculenta* (L.) *Schoot* was purchased from a local farmer market, in Hangzhou, China. The average initial moisture content of the samples was  $4.336 \pm 0.001$  kg water·kg dry matter<sup>-1</sup> (dry basis). At the experiment was the *Colocasia esculenta* (L.) *Schoot* peeled and thinly sliced manually in thicknesses of 0.02 m×0.02 m×0.001 m, 0.02 m×0.02 m×0.002 m and 0.02 m×0.02 m×0.003 m.

### Experimental equipment

The drying experiments were completed in a digital experiment drying tunnel. The tunnel provided the air-flow by a centrifugal fan, regulated the air volume flow with butterfly valves, heated the passing air with an electric heater, controlled the desired temperature of drying air by a proportional controller and showed the quality of sample using a weighing sensor. The rectangle circulation area of tunnel was 0.0256 m<sup>2</sup>, the superficial area of the square drying tray with holes was 0.01 m<sup>2</sup>, the hot air flowed horizontal once passing the tray. The measure accuracy of the temperature, quality and air volume flow control system was 0.1 °C, 0.1 g and 0.1 m<sup>3</sup>·h<sup>-1</sup> respectively. The air velocity was determined with air volume flow divided the circulation area of tunnel. Figure 1 shows the drying tunnel schematic.

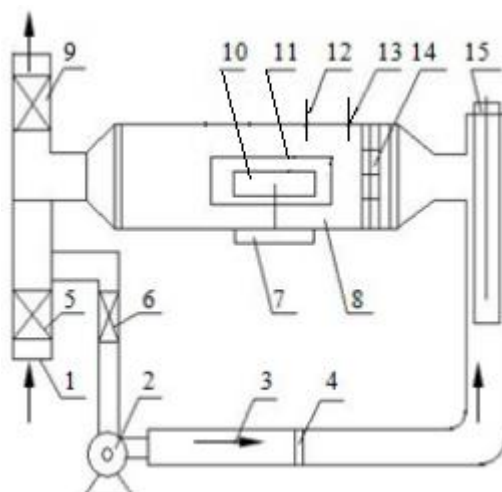


**Figure 1.** Schematic diagram of drying system

1. air intake 2. draught fan 3. pipeline 4. pressure sensor 5, 6. butterfly valve  
7. weighing sensor 8. tunnel dryer 9. butterfly valve 10. material tray  
11. sight glass door 12. wet bulb temperature sensor  
13. dry bulb temperature sensor 14. airflow uniform device 15. heater

## Drying conditions and procedure

In experiments the thickness of *Colocasia esculenta* (L.) *Schoot* slices ranged from 0.001 to 0.003 m. The relative humidity of drying air in tunnel was determined using the dry bulb temperatures of drying air in front of tray and the wet bulb temperatures of drying air behind tray, which was between 28 - 32 %. The temperature (60.0, 65.0, 70.0, 75.0 and 80.0 °C) and air velocity (0.5, 0.75, 1.0, 1.25 and 1.5 m·s<sup>-1</sup>) of drying were set till stabilizing [12, 13]. The sample was weighted and paved a layer to whole tray. The average loading capacity of samples was 0.70, 0.72, 0.70 kg·m<sup>-2</sup> for temperature, velocity, and thickness experiment, respectively. The tray loaded sample was put into the chamber after the stabilization of drying conditions. The quality of sample and corresponding time were recorded as every reduced 0.2 g. When the quality of sample was invariable was the experiment finished. All experiments were repeated twice.

## Modelling of drying curves

In order to observe the characteristics of drying process at different conditions, the curves of moisture ratio versus drying time and dehydration rate versus moisture content were drawn using experiment data. The dry basis moisture content at any time was calculated using equation 1:

$$X_i = \frac{m_i - m_g}{m_g} \quad (1)$$

where  $m_i$ ,  $m_g$  and  $X_i$  are mass of sample at any time (kg), absolute dried mass of sample (kg) and moisture content at any time (kg water·kg dry matter<sup>-1</sup>), respectively.

The dehydration rate was calculated using equation 2:

$$U_i = \frac{m_{i-1} - m_{i+1}}{A(t_{i+1} - t_{i-1})} \quad (2)$$

where  $m_{i-1}$ ,  $m_{i+1}$ ,  $A$ ,  $t_{i-1}$  or  $t_{i+1}$  and  $U_i$  are mass of sample at  $t_{i-1}$  time (kg), mass of sample at  $t_{i+1}$  time (kg), drying contact area (m<sup>2</sup>), drying time (s) and dehydration rate (kg·m<sup>-2</sup>·s<sup>-1</sup>), respectively.

The moisture ratio was calculated using equation 3:

$$MR = \frac{X_i - X^*}{X_0 - X^*} \quad (3)$$

where  $X_0$ ,  $X^*$  and  $MR$  are initial moisture content (kg water·kg dry matter<sup>-1</sup>), equilibrium moisture content (kg water·kg dry matter<sup>-1</sup>, which is moisture content of sample while the mass is invariable at drying) and moisture ratio (dimensionless), respectively.

Experimental results of moisture ratio with drying time were fitted to the most important semi-theoretical models, widely used in the scientific literature to describe the kinetics of the drying process. The selected mathematical models are identified in Table 1.

**Table 1.** Thin-layer drying models applied to drying curves

Model no.	Model name	Model
1	Logarithmic	$MR = a \exp(-kt) + c$
2	Wang and Singh	$MR = 1 + at + bt^2$
3	Modified page	$MR = a \exp(-kt^n)$
4	Page	$MR = \exp(-kt^n)$
5	Henderson and Pabis	$MR = a \exp(-kt)$
6	Newton	$MR = \exp(-kt)$

Non-linear regression techniques were used to obtain the different constants in each selected model. The indexes of coefficient of determination ( $R^2$ ), reduced chi square ( $\chi^2$ ) and root mean square error analysis ( $RMSE$ ) were used to evaluate the degree of each model equation fitted to experimental data. The higher values of the coefficient of determination ( $R^2$ ) and the lower values of the reduced chi-square ( $\chi^2$ ) and the root mean square error analysis ( $RMSE$ ) were chosen for goodness of fit, according to the criterion followed by Menges and Ertekin [13] and by Midilli and Kucuk [14]. The values of  $R^2$  were directly gotten from the drawn drying curve graph, the  $\chi^2$  and  $RMSE$  can be calculated as:

$$\chi^2 = \frac{\sum_{i=1}^N (MR_{\text{exp},i} - MR_{\text{pre},i})^2}{N - z} \quad (4)$$

$$RMSE = \left[ \frac{1}{N} \sum_{i=1}^N (MR_{\text{pre},i} - MR_{\text{exp},i})^2 \right]^{1/2} \quad (5)$$

where  $MR_{\text{exp},i}$ ,  $MR_{\text{pre},i}$ ,  $N$  and  $z$  are experimental moisture ratio (dimensionless), predicted moisture ratio (dimensionless), number of observations and number of constants in the regression model, respectively.

### Calculation of effective moisture diffusivity

The effective moisture diffusivity coefficients were obtained by fitting the experimental drying data using Fick's second law (equation 6).

$$\frac{\partial X}{\partial t} = D_{\text{eff}} \frac{\partial^2 X}{\partial x^2} \quad (6)$$

Crank [15] studied the case of slab geometry for the sample; he supposed that the distribution of initial moisture within sample was uniform, the external resistance for transmitting was negligible, the moisture diffusivity was changeless and the shrinking size of sample during drying process relative to the initial size could be neglected; the solution of equation 6 was obtained as follow (equation 7):

$$MR = \frac{8}{\pi^2} \sum_{n=1}^{\infty} \frac{1}{(2n-1)^2} \exp\left(\frac{-(2n-1)^2 \pi^2 D_{\text{eff}} t}{4H^2}\right) \quad (7)$$

where  $D_{\text{eff}}$ ,  $t$ ,  $H$  and  $n$  are the effective moisture diffusivity ( $\text{m}^2 \cdot \text{s}^{-1}$ ), the drying time (s), half thickness of samples (m) and a positive integer, respectively.

For long time drying process;  $n = 1$ , then equation 7 can be simplified as equation 8:

$$MR = \frac{8}{\pi^2} \exp\left(\frac{-\pi^2 D_{eff} t}{4H^2}\right) \quad (8)$$

Equation 8 can be further linearly expressed to a straight-line equation as equation 9 [5, 7, 16].

$$\ln(MR) = \ln\left(\frac{8}{\pi^2}\right) - \left(\frac{\pi^2 D_{eff} t}{4H^2}\right) \quad (9)$$

From equation 9, a straight line can be drawn by  $\ln(MR)$  versus  $t$  with a slope ( $K$ ) of:

$$K = \frac{\pi^2 D_{eff}}{4H^2} \quad (10)$$

The  $D_{eff}$  are easily calculated by equation 10.

### Estimation of activation energy

The value of activation energy is the characterization of ease degree which the water molecule needs to span the energy obstacle while transmitting within the sample. The relevance of  $D_{eff}$  and  $T$  is usually expressed by the Arrhenius equation (equation 11) [17, 18]:

$$D_{eff} = D_0 \exp\left(\frac{-E_a}{R(T + 273.15)}\right) \quad (11)$$

where  $D_0$ ,  $E_a$ ,  $R$  and  $T$  are the pre-exponential factor of Arrhenius equation ( $m^2 \cdot s^{-1}$ ), the activation energy ( $kJ \cdot mol^{-1}$ ), the universal gas constant ( $kJ \cdot mol^{-1} \cdot K^{-1}$ ) and hot air temperature ( $^{\circ}C$ ), respectively.

## RESULTS AND DISCUSSION

### Drying curves and characteristics

#### *Effect of drying temperature on the drying process*

The *Colocasia esculenta* (L.) Schoot slices of 0.002 m thickness were dried at 60.0, 65.0, 70.0, 75.0 and 80.0  $^{\circ}C$  at 1.0  $m \cdot s^{-1}$  air velocity and 0.70  $kg \cdot m^{-2}$  average loading capacity. The  $MR$  versus  $t$  at the selected temperatures was shown in Figure 2. The  $U_i$  versus  $X_i$  curves was shown in Figure 3.

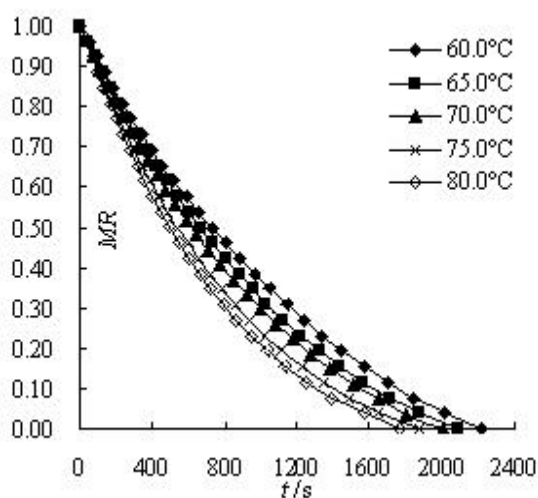


**Figure 2.** The curves of  $MR$  versus  $t$  for temperature

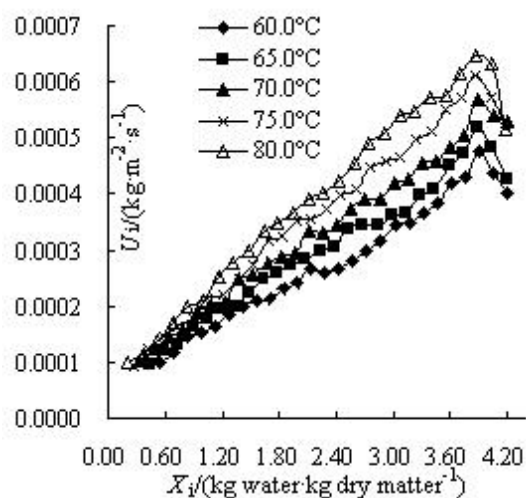


**Figure 3.** The curves of  $U_i$  versus  $X_i$  for temperature

From Figure 2, it could be seen that  $MR$  of samples decreased with the increase of drying time, and an increase in drying air temperature significant resulted in a decrease in the drying time. This might be because heat transfer impetus which was the temperature difference between dry bulb temperature of hot air and wet bulb temperature of material surface increased with the drying temperature increasing, and mass transfer impetus which was the humidity difference between actual humidity of hot air and humidity of material surface also became larger for the reduction of the air relative humidity (from 32 to 28 %). This was in agreement with the earlier research on the drying of agricultural products such as sweet potato [5], yam [10], carrots [11], garlic [12] and seedless grapes [18].

It could be observed from Figure 3 that drying process could be divided into two periods: short accelerating and long falling rate period, there was no constant dehydration rate period. After an initial short period, which actually accorded with the heating up period, the dehydration rate reached a maximum value and then the sample dried following a falling dehydration rate until the equilibrium moisture content was attained. The reason of the constant rate period disappearance during total drying stage might be caused by the fact that at earlier stages of drying process the sample could not constantly provide enough moisture for an appreciable time period due to the loss of free moisture and the shrunk of sample organization structure [18, 19]. The dehydration rate decreased at the subsequent drying period because of the decreased of moisture diffusion rate from inner to outer surface of sample [20]. These results explained that the moisture diffusion was the dominant physical mechanism controlling moisture migration from inner to outer surface of sample. Similar results have been reported in literature by other researchers, such as Doymaz for sweet potato [5], Kaya et al. for carrots [11], and Xiao et al. for seedless grapes [18].



### Effect of air velocity on the drying process

At drying temperature  $70.0\text{ }^{\circ}\text{C}$  and  $0.72\text{ kg}\cdot\text{m}^{-2}$  average loading capacity of *Colocasia esculenta* (L.) Schoot slices  $0.002\text{ m}$  thickness, the influence of air velocity  $0.5$ ,  $0.75$ ,  $1.0$ ,  $1.25$  and  $1.5\text{ m}\cdot\text{s}^{-1}$  on the drying process was separately investigated. The  $MR$  versus  $t$  curves and  $U_i$  versus  $X_i$  curves were shown in Figure 4 and Figure 5, respectively.

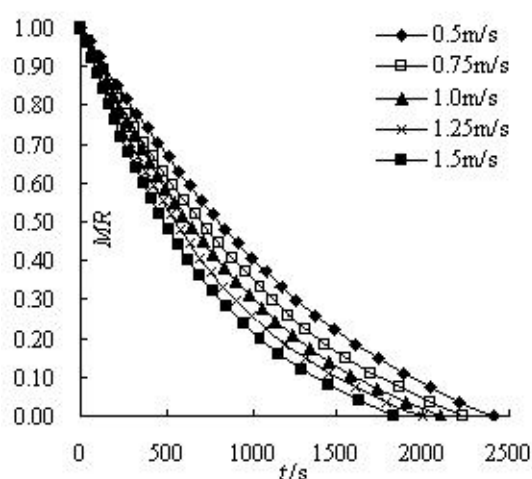


Figure 4. The curves of  $MR$  versus  $t$  for air velocity

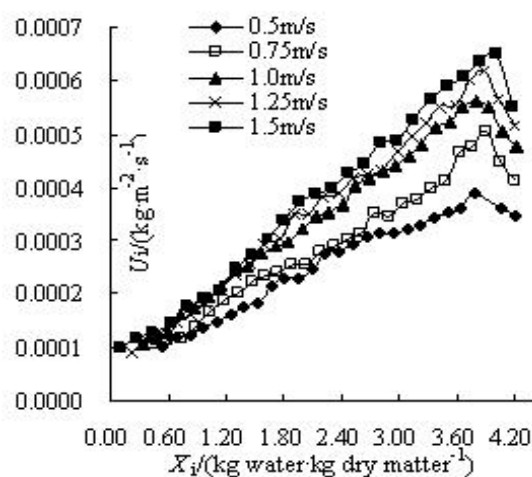


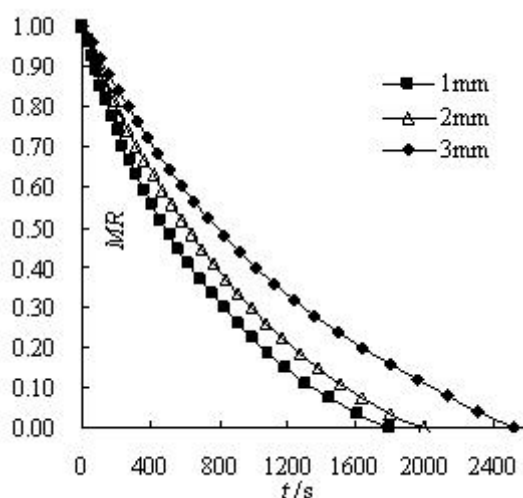
Figure 5. The curves of  $U_i$  versus  $X_i$  for air velocity

As seen in Figure 4, the drying time decreased with the increase of hot air velocity, the reason for this was that the humidity difference, the convective heat and mass transfer coefficient were increased between drying air and sample. The constant dehydration rate period had also not appeared throughout the drying period in Figure 5. The influence of the drying air velocity was significant at the beginning of the process, implying that the evaporation initially took place at the surface, being therefore more directly affected by air velocity. The initial surface evaporation was gradually replaced by an evaporation front that recedes to the interior of the solid. The predominance of air velocity was therefore succeeded by the moisture diffusion process, which became the most important factor. The results were generally in agreement with some of the literature on the drying of various agricultural products [11, 13, 18, 21].

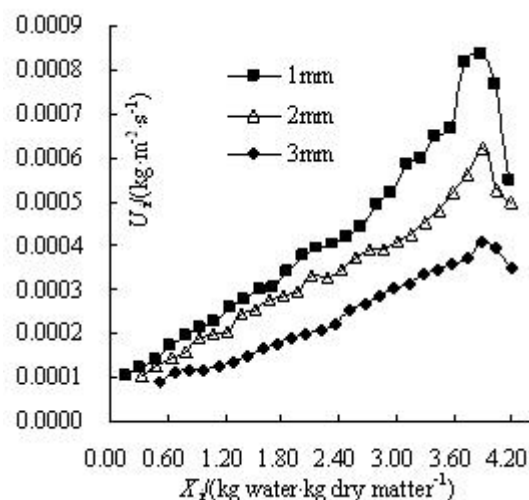
### Effect of sample thickness on the drying process

Figure 6 showed the  $MR$  versus  $t$  curves at  $70.0\text{ }^{\circ}\text{C}$  temperature and  $1.0\text{ m}\cdot\text{s}^{-1}$  air velocity for  $0.001$ ,  $0.002$  and  $0.003\text{ m}$  thickness. The average loading capacity of *Colocasia esculenta* (L.) Schoot slices was  $0.70\text{ kg}\cdot\text{m}^{-2}$ . Figure 7 showed corresponding the  $U_i$  versus  $X_i$  curves. The similarly air temperature and velocity results were observed. The results were generally in agreement with some of the literature on the drying of various agricultural products [11, 12, 22, 23].





**Figure 6.** The curves of MR versus  $t$  for thickness



**Figure 7.** The curves of  $U_i$  versus  $X_i$  for thickness

As seen from Figure 6, the thicker the sample thickness, the longer the drying time required to reach to a certain level of moisture content or equilibrium moisture content. The thickness of sample slices was found to be an important influence factor to drying time. Result showed that the drying time lengthened with the increased of the thickness of sample, this was because of the distance of moisture transfer from inner to surface rising. The similar observation was found by Kaya *et al.* for carrots [11], Rasouli *et al.* for garlic [22].

It was observed that a drying constant rate period was also not detected in the dehydration rate curves (Figure 7). After an initial short accelerating rate period, the drying took place in a longer falling rate period, which indicated that the moisture diffusion was the dominant physical mechanism controlling moisture migration in *Colocasia esculenta* (L.) Shoot slices. This result was in agreement with previous literature studies on drying of agricultural products [11, 23].

At the same time, Figure 7 showed that the dehydration rate in thickness of 0.001 m was highest. Thinly sliced sample dried faster due to the decreased of the moisture transmitted distance and the increased of the exposed surface area in drying air for a same sample volume. The similar observation was found by Rasouli *et al.* for garlic drying [22] and Doymaz for leek drying [23].

## Drying kinetic model and coefficient

### Modelling of drying curves

The six thin-layer drying models in Table 1 were compared in terms of the statistical parameters  $R^2$ ,  $\chi^2$  and RMSE. The statistical analysis values were summarized in Table 2.

**Table 2.** The fitting models and statistical results of models at different drying conditions

Model no.	Conditions		Model constants	$R^2$	$\chi^2$	RMSE
1	T [°C]	60.0	$a = 1.2193, k = 0.0006740, c = -0.2925$	0.9999	0.000013	0.003353
		65.0	$a = 1.2483, k = 0.0007963, c = -0.2405$	0.9998	0.000014	0.003493
		70.0	$a = 1.2193, k = 0.0008712, c = -0.2155$	0.9999	0.000005	0.002091
		75.0	$a = 1.1691, k = 0.0010825, c = -0.1555$	0.9999	0.000014	0.003492
		80.0	$a = 1.1545, k = 0.0012136, c = -0.1350$	0.9999	0.000024	0.004570
	V [m·s <sup>-1</sup> ]	0.5	$a = 1.2959, k = 0.0006422, c = -0.2754$	0.9998	0.000037	0.005753
		0.75	$a = 1.2342, k = 0.0007578, c = -0.2285$	0.9998	0.000010	0.002946
		1.0	$a = 1.1922, k = 0.0009158, c = -0.1755$	0.9999	0.000015	0.003634
		1.25	$a = 1.1358, k = 0.0010914, c = -0.1237$	0.9999	0.000011	0.003075
		1.5	$a = 1.1086, k = 0.0012366, c = -0.1056$	0.9998	0.000011	0.003144
	H [m]	0.001	$a = 1.1244, k = 0.0011563, c = -0.1385$	0.9997	0.000076	0.008234
		0.002	$a = 1.2043, k = 0.0009043, c = -0.1985$	0.9999	0.000012	0.003327
		0.003	$a = 1.2395, k = 0.0006252, c = -0.2515$	0.9995	0.000060	0.007260
2	T [°C]	60.0	$a = -0.0007988, b = 1.612 \times 10^{-7}$	0.9986	0.000126	0.010781
		65.0	$a = -0.0008771, b = 1.954 \times 10^{-7}$	0.9991	0.000075	0.008323
		70.0	$a = -0.0009409, b = 2.272 \times 10^{-7}$	0.9986	0.000112	0.010202
		75.0	$a = -0.0010674, b = 2.944 \times 10^{-7}$	0.9981	0.000141	0.011409
		80.0	$a = -0.0011535, b = 3.440 \times 10^{-7}$	0.9981	0.000142	0.011440
	V [m·s <sup>-1</sup> ]	0.5	$a = -0.0007183, b = 1.284 \times 10^{-7}$	0.9997	0.000021	0.004443
		0.75	$a = -0.0008290, b = 1.758 \times 10^{-7}$	0.9987	0.000099	0.009594
		1.0	$a = -0.0009240, b = 2.200 \times 10^{-7}$	0.9987	0.000094	0.009356
		1.25	$a = -0.0010357, b = 2.790 \times 10^{-7}$	0.9970	0.000225	0.014448
		1.5	$a = -0.0011605, b = 3.515 \times 10^{-7}$	0.9949	0.000395	0.019069
	H [m]	0.001	$a = -0.0011694, b = 3.580 \times 10^{-7}$	0.9927	0.000607	0.023722
		0.002	$a = -0.0009531, b = 2.340 \times 10^{-7}$	0.9981	0.000155	0.011983
		0.003	$a = -0.0007315, b = 1.389 \times 10^{-7}$	0.9969	0.000254	0.015296
3	T [°C]	60.0	$a = 0.9885, k = 0.00028324, n = 1.1928$	0.9943	0.000479	0.020533
		65.0	$a = 0.9892, k = 0.00031060, n = 1.1948$	0.9951	0.000375	0.018162
		70.0	$a = 0.9876, k = 0.00037537, n = 1.1776$	0.9958	0.000315	0.016698
		75.0	$a = 0.9898, k = 0.00041952, n = 1.1824$	0.9973	0.000186	0.012801
		80.0	$a = 0.9938, k = 0.00047805, n = 1.1767$	0.9980	0.000139	0.011050
	V [m·s <sup>-1</sup> ]	0.5	$a = 0.9880, k = 0.00015899, n = 1.2576$	0.9962	0.000272	0.015469
		0.75	$a = 0.9892, k = 0.00028304, n = 1.1977$	0.9959	0.000327	0.017006
		1.0	$a = 0.9900, k = 0.00029628, n = 1.2093$	0.9974	0.000197	0.013256
		1.25	$a = 0.9947, k = 0.00050382, n = 1.1490$	0.9981	0.000128	0.010625
		1.5	$a = 0.9942, k = 0.00065932, n = 1.1269$	0.9983	0.000100	0.009363
	H [m]	0.001	$a = 0.9982, k = 0.00081600, n = 1.0977$	0.9956	0.000281	0.015776
		0.002	$a = 0.9895, k = 0.00039588, n = 1.1722$	0.9956	0.000333	0.017159
		0.003	$a = 0.9989, k = 0.00054802, n = 1.0422$	0.9993	0.000038	0.005798

T = drying air temperature, V = air velocity, H = slices thickness

**Table 2.** The fitting models and statistical results of models at different drying conditions (continuation)

Model no.	Conditions		Model constants	$R^2$	$\chi^2$	RMSE
4	T [°C]	60.0	$k = 0.00043725, n = 1.1313$	0.9928	0.000562	0.022733
		65.0	$k = 0.00046383, n = 1.1373$	0.9938	0.000462	0.020625
		70.0	$k = 0.00059819, n = 1.1100$	0.9938	0.000428	0.019878
		75.0	$k = 0.00060221, n = 1.1292$	0.9966	0.000228	0.014498
		80.0	$k = 0.00058799, n = 1.1460$	0.9978	0.000153	0.011854
	V [m·s <sup>-1</sup> ]	0.5	$k = 0.00026576, n = 1.1857$	0.9934	0.000391	0.018974
		0.75	$k = 0.00042748, n = 1.1392$	0.9950	0.000386	0.018882
		1.0	$k = 0.00043564, n = 1.1536$	0.9966	0.000228	0.014542
		1.25	$k = 0.00060197, n = 1.1230$	0.9978	0.000138	0.011296
		1.5	$k = 0.00079061, n = 1.1001$	0.9983	0.000104	0.009752
	H [m]	0.001	$k = 0.00086170, n = 1.0897$	0.9958	0.000270	0.015783
		0.002	$k = 0.00058080, n = 1.1116$	0.9947	0.000394	0.019071
		0.003	$k = 0.00043023, n = 1.1164$	0.9953	0.000329	0.017374
5	T [°C]	60.0	$a = 1.2061, k = 0.0013699$	0.9466	0.006248	0.075942
		65.0	$a = 1.2065, k = 0.0014959$	0.9539	0.006038	0.076133
		70.0	$a = 1.1916, k = 0.0015726$	0.9576	0.005176	0.070598
		75.0	$a = 1.1752, k = 0.0017397$	0.9676	0.004109	0.061589
		80.0	$a = 1.1720, k = 0.0018660$	0.9736	0.003654	0.058080
	V [m·s <sup>-1</sup> ]	0.5	$a = 1.2604, k = 0.0012840$	0.9486	0.007779	0.084739
		0.75	$a = 1.1998, k = 0.0013972$	0.9577	0.005060	0.071133
		1.0	$a = 1.1985, k = 0.0015422$	0.9634	0.004791	0.066786
		1.25	$a = 1.1548, k = 0.0016406$	0.9739	0.003080	0.053400
		1.5	$a = 1.1246, k = 0.0017727$	0.9793	0.002110	0.044061
	H [m]	0.001	$a = 1.1223, k = 0.0017928$	0.9722	0.002346	0.047528
		0.002	$a = 1.2031, k = 0.0015933$	0.9580	0.005729	0.074278
		0.003	$a = 1.1673, k = 0.0011850$	0.9566	0.003759	0.060119
6	T [°C]	60.0	$k = 0.0012167$	0.9283	0.003726	0.059856
		65.0	$k = 0.0013288$	0.9356	0.003698	0.060813
		70.0	$k = 0.0014090$	0.9414	0.003232	0.055785
		75.0	$k = 0.0015723$	0.9535	0.002715	0.051090
		80.0	$k = 0.0016904$	0.9599	0.002603	0.050026
	V [m·s <sup>-1</sup> ]	0.5	$k = 0.0011114$	0.9233	0.004884	0.068531
		0.75	$k = 0.0012464$	0.9404	0.003413	0.057326
		1.0	$k = 0.0013783$	0.9464	0.003259	0.056098
		1.25	$k = 0.0015001$	0.9625	0.002138	0.045369
		1.5	$k = 0.0016473$	0.9714	0.001450	0.037306
	H [m]	0.001	$k = 0.0016689$	0.9647	0.001386	0.036532
		0.002	$k = 0.0014200$	0.9434	0.002997	0.053723
		0.003	$k = 0.0010746$	0.9435	0.002554	0.049518

T = drying air temperature, V= air velocity, H = slices thickness

In all cases, the  $R^2$  values varied between 0.9233 and 0.9999,  $\chi^2$  values between 0.000010 and 0.007779, and  $RMSE$  values between 0.002091 and 0.084739. Generally, Logarithmic model similarly gave a higher average  $R^2$  and lower average  $\chi^2$  and average  $RMSE$  values for different temperature, air velocity and thickness. Thus, it was selected to represent the thin-layer drying characteristics of *Colocasia esculenta* (L.) *Schoot*.

### Effective moisture diffusivity

The values of effective moisture diffusivity at different conditions were calculated using equation 10 and were shown in Table 3. The effective diffusivities of *Colocasia esculenta* (L.) *Schoot* at 60.0 - 80.0 °C ranged from  $4.94 \times 10^{-10}$  to  $6.86 \times 10^{-10} \text{ m}^2 \cdot \text{s}^{-1}$  and the values of diffusivities increased with the increase of temperature. The reason was that the activity of water molecules was increased with drying temperature raise leading to the raise of moisture diffusion ability [18]. The  $D_{\text{eff}}$  values varied in the range of  $4.51 \times 10^{-10}$  to  $6.68 \times 10^{-10}$  at 0.5 - 1.5  $\text{m} \cdot \text{s}^{-1}$  of air velocity and the values of diffusivities also increased with the increase of velocity. This result was due to the increase of the mass transmission coefficient with increasing of air velocity, leading to enhance mass transmission rate and moisture migration from inside to outside. Similar observations have earlier been reported in literature [11, 18, 21]. The  $D_{\text{eff}}$  values varied between  $1.69 \times 10^{-10}$  and  $9.81 \times 10^{-10} \text{ m}^2 \cdot \text{s}^{-1}$  at 0.001 - 0.003 m of thickness, respectively and it also increased with the increase of thickness. This reason was estimated that the moisture concentration difference between inner and surface of material raised with the increase of thickness, and the internal moisture transfer occurred along a longer distance compared to lower thickness. The results were generally in agreement with some of the literature [11, 23]. These values meet the standard range for agribusiness and agricultural products (from  $10^{-10} \text{ m}^2 \cdot \text{s}^{-1}$  to  $10^{-9} \text{ m}^2 \cdot \text{s}^{-1}$ ), and can be compared to  $1.82 \times 10^{-10}$  to  $5.84 \times 10^{-10} \text{ m}^2 \cdot \text{s}^{-1}$  for seedless grapes [18],  $2.524 \times 10^{-10}$  to  $7.566 \times 10^{-10} \text{ m}^2 \cdot \text{s}^{-1}$  for garlic [22],  $1.32 \times 10^{-10}$  to  $1.09 \times 10^{-9} \text{ m}^2 \cdot \text{s}^{-1}$  for onion [24].

**Table 3.** The effective moisture diffusion coefficient of different factor

Factor		$D_{\text{eff}} \times 10^{10} [\text{m}^2 \cdot \text{s}^{-1}]$
T [°C]	60.0	4.94
	65.0	5.39
	70.0	5.72
	75.0	6.38
	80.0	6.86
V [ $\text{m} \cdot \text{s}^{-1}$ ]	0.5	4.51
	0.75	5.06
	1.0	5.59
	1.25	6.09
	1.5	6.68
H [m]	0.001	1.69
	0.002	5.76
	0.003	9.81

### Activation energy

Equation 11 could be rearranged in the form of equation 12:

$$\ln(D_{eff}) = \ln(D_0) - \frac{E_a}{R(T + 273.15)} \quad (12)$$

Values of  $D_{eff}$  calculated by equation 12 for experiments were plotted in Figure 8. The plot was found to be essentially a straight line in the range of temperatures investigated, indicating Arrhenius dependence. From the slope of the straight line, the activation energy was found to be  $16.15 \text{ kJ} \cdot \text{mol}^{-1}$ . This result was similar to those given in the literature for drying of different agricultural products:  $12.43 \text{ kJ} \cdot \text{mol}^{-1}$  for olive-waste cake [25];  $11.38 \text{ kJ} \cdot \text{mol}^{-1}$  for sweet potato [26];  $21.30 \text{ kJ} \cdot \text{mol}^{-1}$  for wet olive husk [27];  $22.48 \text{ kJ} \cdot \text{mol}^{-1}$  for green pea [28].

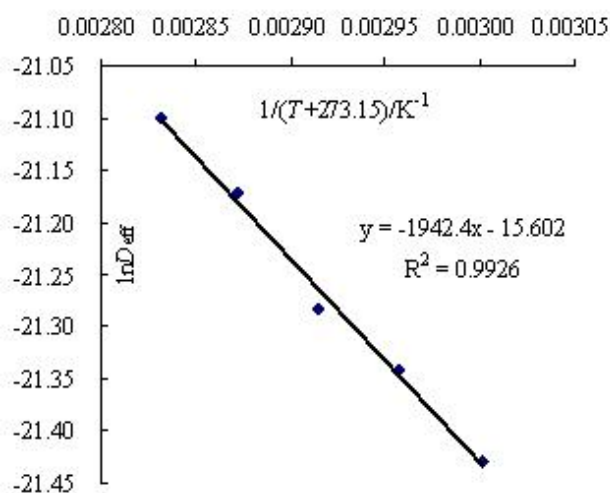


**Figure 8.** The relationship of  $\ln D_{eff}$  and  $1/(T+273.15)$

### CONCLUSIONS

The increase in air temperature and air velocity and the decrease in sample thickness significantly reduced the drying time of the *Colocasia esculenta* (L.) Schoot under the experimental carried out in a tunnel dryer with forced convection mode. Moreover, it was observed that the dehydration rate increased quite significantly as drying temperature and air velocity were raised and as sample thickness was thinned, hence reducing drastically the total drying time. Drying curves of *Colocasia esculenta* (L.) Schoot did not show a constant rate period and showed a falling rate-drying period after a momentary accelerating rate period. Goodness of fit of the experimental data by six thin-layer drying models was determined by comparing determination of coefficient  $R^2$ , reduced  $\chi^2$  and root mean square error  $RMSE$ . The Logarithmic empirical model (values of  $R^2$  over 0.9995,  $\chi^2$  under 0.000076 and  $RMSE$  under 0.008234 along the whole range) showed a good fit for all curves than the other models. The values of effective diffusivity varied from  $4.94 \times 10^{-10}$  to  $6.86 \times 10^{-10} \text{ m}^2 \cdot \text{s}^{-1}$  for drying at the researched air temperature range of 60.0 to 80.0 °C and fixed other drying conditions; for drying at

0.5 - 1.5 m·s<sup>-1</sup> of air velocity and fixed air temperature and slices thickness varied from 4.51×10<sup>-10</sup> to 6.68×10<sup>-10</sup> m<sup>2</sup>·s<sup>-1</sup>; for drying at the researched slices thickness range of 0.001 - 0.003 m and fixed air temperature and air velocity varied from 1.69×10<sup>-10</sup> to 9.81×10<sup>-10</sup> m<sup>2</sup>·s<sup>-1</sup>. The effective diffusivity increased with rising of the air temperature, air velocity and sample thickness. Temperature dependence of the diffusivity coefficients was described by Arrhenius-type relationship. The activation energy for moisture diffusion was found as 16.15 kJ·mol<sup>-1</sup>, which was in agreement with data in the literature.

## REFERENCES

1. Sefa-Dedeh, S., Agyir-Sackey, E.K.: Chemical Composition and the Effect of Processing on Oxalate Content of Cocoyam *Xanthosoma Sagittifolium* and Colocasia *Esculenta* Cormels, *Food Chemistry*, **2004**, 85 (4), 479-487;
2. Huang, C.C., Chen, W.C., Wang, C.C.R.: Comparison of Taiwan Paddy- and Upland-cultivated Taro (*Colocasia esculenta* L.) Cultivars for Nutritive Values, *Food Chemistry*, **2007**, 102 (1), 250-256;
3. Gonçalves, R.F., Silva, A.M.S., Silva, A.M., Valentão, P.C., Ferreres, F., Gil-Izquierdo, A., Silva, J.B., Santos, D., Andrade, P.B.: Influence of Taro (*Colocasia Esculenta* L. Shott) Growth Conditions on the Phenolic Composition and Biological Properties, *Food Chemistry*, **2013**, 141 (4), 3480-3485;
4. Mishra, A.K., Sharma, K., Misra, R.S.: Purification and Characterization of Elicitor Protein from *Phytophthora Colocasiae* and Basic Resistance in *Colocasia Esculenta*, *Microbiological Research*, **2009**, 164 (6), 688-693;
5. Doymaz, I.: Thin-layer Drying Characteristics of Sweet Potato Slices and Mathematical Modelling, *Heat and Mass Transfer*, **2011**, 47 (3), 277-285;
6. Doymaz, I., Ismail, O.: Drying Characteristics of Sweet Cherry, *Food and Bioproducts Processing*, **2011**, 89 (1), 31-38;
7. Singh, S.P., Jairaj, K.S., Srikant, K.: Universal Drying Rate Constant of Seedless Grapes: A Review, *Renewable & Sustainable Energy Reviews*, **2012**, 16 (8), 6295-6302;
8. Sacilik, K., Keskin, R., Elicin, A.K.: Mathematical Modelling of Solar Tunnel Drying of Thin Layer Organic Tomato, *Journal of Food Engineering*, **2006**, 73 (3), 231-238;
9. Leeratanarak, N., Devahastin, S., Chiewchan, N.: Drying Kinetics and Quality of Potato Chips Undergoing Different Drying Techniques, *Journal of Food Engineering*, **2007**, 77 (3), 635-643;
10. Sobukola, O.P., Dairo, O.U., Odunewu, A.V.: Convective Hot Air Drying of Blanched Yam Slices, *International Journal of Food Science & Technology*, **2008**, 43 (7), 1233-1238;
11. Kaya, A., Aydın, O., Demirtaş, C.: Experimental and Theoretical Analysis of Drying Carrots, *Desalination*, **2009**, 237 (1), 285-295;
12. Madamba, P.S., Driscoll, R.H., Buckle, K.A.: Thin-layer Drying Characteristics of Garlic Slices, *Journal of Food Engineering*, **1996**, 29 (1), 75-97;
13. Menges, H.O., Ertekin, C.: Mathematical Modelling of Thin Layer Drying of Golden Apples, *Journal of Food Engineering*, **2006**, 77 (1), 119-125;
14. Midilli, A., Kucuk, H.: Mathematical Modelling of Thin Layer Drying of Pistachio by using Solar Energy, *Energy Conversion and Management*, **2003**, 44 (7), 1111-1122;
15. Crank, J.: The Mathematics of Diffusion. Clarendon Press, Oxford, 1975;
16. Evin, D.: Thin Layer Drying Kinetics of *Gundelia Tournfortii* L, *Food and Bioproducts Processing*, **2012**, 90 (2), 323-332;
17. Özbek, B., Dadali, G.: Thin-layer Drying Characteristics and Modelling of Mint Leaves Undergoing Microwave Treatment, *Journal of Food Engineering*, **2008**, 83 (4), 541-549;
18. Xiao, H.W., Pang, C.L., Wang, L.H., Bai, J.W., Yang, W.X., Gao, Z.J.: Drying Kinetics and Quality of Monukka Seedless Grapes Dried in An Air-impingement Jet Dryer, *Biosystems Engineering*, **2010**, 105 (2), 233-240;



19. Singh, B., Gupta, A.K.: Mass Transfer Kinetics and Determination of Effective Diffusivity during Convective Dehydration of Pre-osmosed Carrot Cubes, *Journal of Food Engineering*, **2007**, 79 (2), 459-470;
20. Kumar, N., Sarkar, B.C., Sharma, H.K.: Mathematical Modelling of Thin Layer Hot Air Drying of Carrot Pomace, *Journal of Food Science and Technology*, **2012**, 49 (1), 33-41;
21. Babalis, S.J., Papanicolaou, E., Kyriakis, N., Belessiotis, V.G.: Evaluation of Thin-layer Drying Models for Describing Drying Kinetics of Figs (*Ficus carica*), *Journal of Food Engineering*, **2006**, 75 (2), 205-214;
22. Rasouli, M., Seiedlou, S., Ghasemzadeh, H.R., Nalbandi, H.: Influence of Drying Conditions on the Effective Moisture Diffusivity and Energy of Activation during the Hot Air Drying of Garlic, *Australian Journal of Agricultural Engineering*, **2011**, 2 (4), 96-101;
23. Doymaz, I.: Influence of Blanching and Slice Thickness on Drying Characteristics of Leek Slices, *Chemical Engineering and Processing: Process Intensification*, **2008**, 47 (1), 41-47;
24. Mitra, J., Shrivastava, S.L., Srinivasa, R.P.: Vacuum Dehydration Kinetics of Onion Slices, *Food and Bioproducts Processing*, **2011**, 89 (1), 1-9;
25. Vega-Gálvez, A., Miranda, M., Díaz, L.P., Lopez, L., Rodriguez, K., Scala, K.D.: Effective Moisture Diffusivity Determination and Mathematical Modeling of the Drying Curves of the Olive-waste Cake, *Bioresource Technology*, **2010**, 101 (19), 7265-7270;
26. Singh, N.J., Pandey, R.K.: Convective Air Drying Characteristics of Sweet Potato Cube (*Ipomoea Batatas* L.), *Food and Bioproducts Processing*, **2012**, 90 (2), 317-322;
27. Ruiz Celma, A., Rojas, S., Lopez-Rodríguez, F.: Mathematical Modelling of Thin-layer Infrared Drying of Wet Olive Husk, *Chemical Engineering and Processing: Process Intensification*, **2008**, 47 (9), 1810-1818;
28. Pardeshi, I.L., Arora, S., Borker, P.A.: Thin-layer Drying of Green Peas and Selection of A Suitable Thin-layer Drying Model, *Dry Technology*, **2009**, 27 (2), 288-295.